# Identification of Novel 2-(1*H*-Indol-1-yl)benzohydrazides CXCR4 Ligands Impairing Breast Cancer Growth and Motility

Fedora Grande[1*#], Ines Barone[1#], Francesca Aiello[1], Andrea Brancale[2], Michela Cancellieri[2], Mariateresa Badolato[1], Francesca Chemi[1], Cinzia Giordano[3], Valentina Vircillo[1], Daniela Bonofiglio[1], Antonio Garofalo[1], Sebastiano Andò[1], Stefania Catalano[1].

[1]Department of Pharmacy, Health and Nutritional Sciences, University of Calabria, Via P. Bucci, 87036 Rende (Cs), Italy.

[2]School of Pharmacy and Pharmaceutical Sciences, Cardiff University, King Edward VII Avenue, Cardiff, CF10 3NB, UK

[3]Centro Sanitario, University of Calabria, Via P. Bucci, 87036 Rende (Cs), Italy.

[#]Authors contributed equally.

*Author for correspondence:

Fedora Grande Tel.: +39 0984 493019; Fax: +39 0984 493118, E-mail: fedora.grande@unical.it

**Background**: Stromal-derived-factor-1 (SDF-1) and the G-protein-coupled-receptor CXCR4 are involved in several physiological and pathological processes including breast cancer spread and progression. Several CXCR4 antagonists have currently reached advanced development stages as potential therapeutic agents for different diseases. **Results**: A small series of novel CXCR4 ligands, based on a 2-(1*H*-indol-1-yl)-benzohydrazide scaffold, have been designed and synthesized. Their orientation into CXCR4 active site was predicted by molecular docking and confirmed by whole cell-based [$^{125}$I]-SDF-1 ligand competition binding assays. One of the synthesized compounds was particularly active in blocking SDF-1-induced breast cancer cell motility, proliferation and downstream signaling activation in different breast cancer cell models and co-

culture systems. **Conclusion**: The newly synthesized compounds represent suitable leads for the development of innovative therapeutic agents targeting CXCR4.

CXCR4 (C-X-C chemokine receptor type 4), also known as CD184 (cluster of differentiation 184) or fusin, is a seven transmembrane G-protein coupled receptor (GPCR) belonging to rhodopsin-like GPCR family [1,2]. CXCR4, first identified as one of the two co-receptors required for the fusion of HIV envelope with the membrane of the targeted cell, was found to be widely expressed in the hematopoietic and immune systems, where it is likely involved in several physiological and pathological processes [3,4].

The natural CXCR4 ligand was recognized to be the Stromal Derived Factor-1 (SDF-1), an eight-kDa homeostatic chemokine peptide also known as CXCL12, which promotes chemotaxis after binding the receptor [5]. The SDF-1/CXCR4 interaction plays a key role in pathological processes, such as HIV infection, inflammation and cancer onset and progression, thus representing an appealing target for the development of innovative broad-spectrum therapeutics [6,7].

The mounting evidence of the crucial role played by CXCR4 in several diseases has encouraged the development of compounds that are able to modulate its biological activity. In the past few years, numerous compounds belonging to different chemical classes, have demonstrated capacity to block SDF-1/CXCR4 interaction (**Figure 1**). Some of these compounds are currently under clinical trials for the treatment of various diseases including cancers, hematologic and vascular diseases, HIV infection, and other immune system disorders involving the modulation of the SDF-1/CXCR4 axis, such as rheumatoid arthritis and lupus [8].

The first identified CXCR4 antagonists were peptide derivatives that, despite the unfavorable pharmacokinetics and metabolic instability, have been the starting point for building up a pharmacophore model subsequently adopted for the design of simpler non-peptide antagonists [8,9]

Among the non-peptide ligands, a macrocyclic "bicyclam" derivative, called AMD3100, also known as Plerixafor (**1**), has been the first CXCR4 antagonist approved by the FDA for diseases involving the mobilization of hematopoietic stem cells [10] and presently it is in advanced clinical trials for other pathological conditions [11-15]. Despite the noteworthy potency, the clinical applicability of this compound is yet limited by a poor bioavailability due to its high overall positive charge at physiologic pH.

Furthermore, the small molecule AMD070 (**2**), the lead of a series of compounds containing at the same time a benzimidazole and a tetrahydroquinoline moiety in their structure, demonstrated a remarkable antagonistic activity after oral administration and it is currently under advanced clinical investigation for the prophylaxis of HIV infection [16-18].

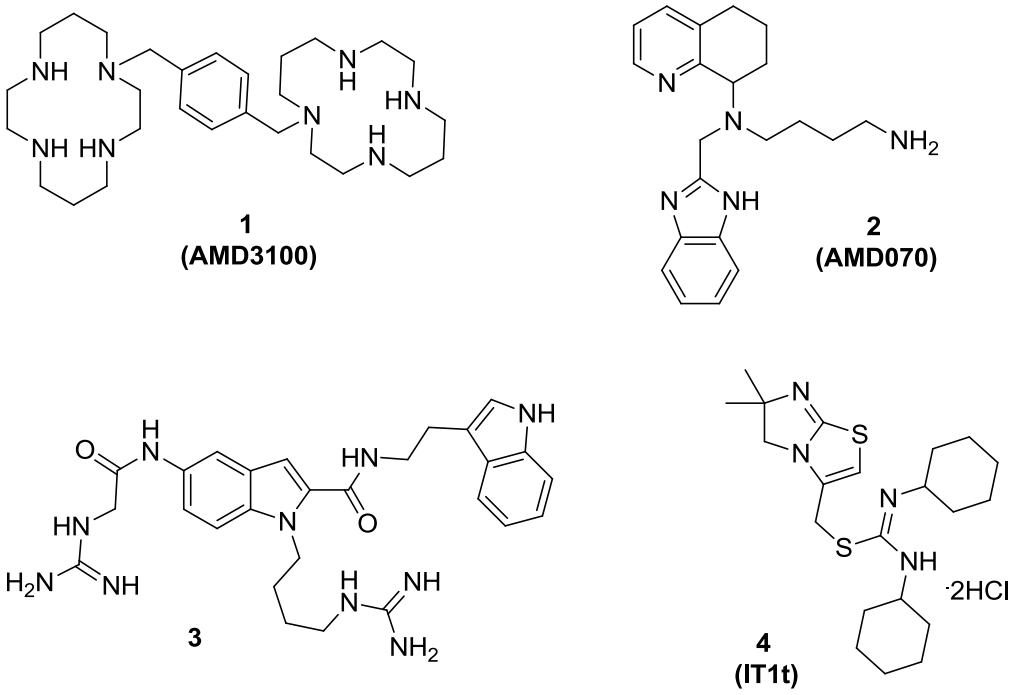


**Figure 1. Chemical structures of known antagonists of CXCR4.**

The evolution in the search of alternative structure for CXCR4 antagonists brought to the identification of poly-substituted indoles, among them compound **3** represents the most promising prototype active in human CXCR4 transfected Chinese hamster ovary (CHO) cells in a [$^{125}$I]-SDF-1 radio-ligand assay [19].

These compounds were abandoned due to their high protonation degree 'in vivo', which precludes an adequate tissues distribution. However, various groups functionalizing the indole nucleus could yet guarantee spatial requirements for key interactions in the previously reported pharmacophore model, as shown by molecular modeling [20]. A further improvement in the definition of CXCR4 receptor was the discovery of the orally active isothiourea ligand IT1t (**4**), which was co-crystallized with the receptor [21,22].

Herein, we report the identification of a small series of CXCR4 antagonists based on a 2-(1*H*-indol-1-yl)-*N*'-arylbenzohydrazide moiety (FIL1-3, **Figure 2**) with typical small molecule drug characteristics reflecting potential favorable pharmacokinetics and many possibilities to be optimized.

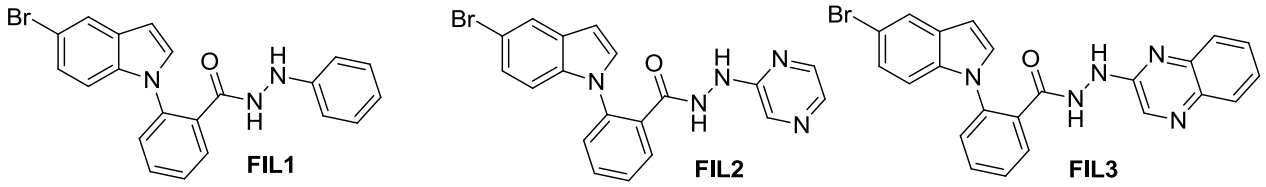


**Figure 2. Structures of studied compounds.**

Since the chemokine SDF-1α and its cognate receptor CXCR4 play a crucial role in breast cancer spread and progression [23,24], the effects of synthesized compounds have been tested in different breast cancer cell models and in co-culture systems by using specific biological assays, such as cell proliferation and wound-healing assays, where they revealed interesting anticancer properties.

In particular, one of the tested compounds, FIL2, was particularly active in blocking SDF-1α-dependent cell motility, proliferation and downstream signaling activation in estrogen-receptor negative and positive breast cancer cells as well as in experimental cell models for acquired endocrine resistance. A specific [$^{125}$I]-SDF-1α binding assay has confirmed that the above properties were unambiguously due to CXCR4 inhibition. This compound was also able to inhibit the effects of cancer-associated fibroblasts (CAFs), key players in the breast tumor microenvironment, on cancer progression.

Based on all the promising results we obtained, the newly synthesized compounds could be considered leads for the development of new selective CXCR4 antagonists as novel tools for the treatment of breast cancer and other CXCR4-related diseases.

## MATERIALS AND METHODS

### Molecular modelling and docking simulations

The molecular modelling simulations were performed on an Apple Mac pro 2.66 GHz Quad-Core Intel Xeon, Running Ubuntu 12.04. The CXCR4 protein was downloaded from the Protein Data Bank, accession code: 3ODU [20] and prepared using the Protein Preparation Wizard tool of Maestro [25]. Putative inhibitors were built and prepared in Maestro and docked with GLIDE, using the SP mode. Images were created using MOE [26].

### Chemical synthesis

General experimental information is reported in ref. 27. The purity of FIL1-3 was > 96 %, as determined by HPLC.

#### *2-(5-Bromo-1H-indol-1-yl)-N'-phenylbenzohydrazide (FIL1)*

To a stirred solution of 2-(5-bromo-1*H*-indol-1-yl)benzoic acid **1** [27] (0.060 g; 0.190 mmol) in DMF (1 mL) CDI (0.031; 0.190 mmol) was added in 10 min. A solution of phenylhydrazine (0.020 g; 0.190 mmol) in DMF (1 mL) was slowly added in 15 min. The reaction mixture was heated to 60°C for 8 hours. The solvent was then evaporated and the solid residue obtained was taken up into ethyl acetate. The resulting solution was sequentially debated with 5% HCl solution and brine. After evaporation of the solvent, the crude product was purified by column chromatography (toluene/ethyl acetate/methanol/ammonium hydroxide, 10/1/1/0.25, as eluent). The title compound was separated as an orange amorphous solid in 22% yield. $^{1}$H NMR (300 MHz, MeOD) δ 7.82 (s, 1H), 7.69-7.60 (m, 3H), 7.44-7.37 (m, 3H), 7.24-7.06 (m, 5H), 7.01-6.81 (m, 2H). $^{13}$C NMR (75 MHz, MeOD) δ 164.0, 148.8, 144.7, 143.9, 142.8, 136.6, 135.9, 130.6, 130.2, 129.4, 129.0,

129.9, 128.8, 128.5, 128.2, 128.0, 127.9, 125.9, 120.4, 118.9, 112.6. HRMS calcd for $C_{21}H_{16}BrN_3O$ 405.0477, found 405.0420. IR (KBr) $\nu_{max}$: 1676 $cm^{-1}$.

***2-(5-Bromo-1H-indol-1-yl)-N'-(pyrazin-2-yl)benzohydrazide (FIL2)***

This compound was prepared following the procedure applied for FIL1 starting from pyrazin-2-yl-hydrazine (0.021 g; 0.190 mmol). The pure compound was obtained as a brown amorphous solid in 50% yield. $^1$H NMR (300 MHz, MeOD) δ 8.11 (s, 1H), 7.99-7.88 (m, 2H), 7.73-7.62 (m, 3H), 7.67 (t, 1H, *J* = 7.6 Hz), 7.44 (d, 1H, *J* = 7.9 Hz), 7.29 (d, 1H, *J* = 3.2 Hz), 7.20-7.09 (m, 1H), 6.97 (d, 1H, *J* = 4.7 Hz), 6.58 (d, 1H, *J* = 3.2 Hz). $^{13}$C NMR (75 MHz, MeOD) δ 167.0, 140.8, 137.8, 135.9, 133.0, 131.3, 130.5, 130.2, 129.9, 128.7, 128.2, 128.0, 127.8, 127.7, 124.5, 124.2, 122.9, 110.9, 102.3. HRMS calcd for $C_{19}H_{14}BrN_5O$ 407.0382 found 407.0407. IR (KBr) $\nu_{max}$: 1656 $cm^{-1}$.

***2-(5-Bromo-1H-indol-1-yl)-N'-(quinoxalin-2-yl)benzohydrazide (FIL3)***

This compound was prepared following the procedure applied for FIL1 starting from quinoxalin-2-yl-hydrazide (0.030 g; 0.190 mmol). The pure compound was obtained as a purple solid in 37% yield. $^1$H NMR (300 MHz, MeOD) δ 8.32 (d, 1H, *J* = 7.5 Hz), 8.10 (d, 1H, *J* = 9.1 Hz), 7.82 (d, 1H, *J* = 9.1 Hz), 7.79-7.69 (m, 2H), 7.55 (t, 2H, *J* = 7.7 Hz), 7.42-7.35 (m, 3H), 7.20-7.05 (m, 3H), 6.59 (d, 1H, *J* = 3.2 Hz). $^{13}$C NMR (75 MHz, MeOD) δ 159.5, 158.0, 137.3, 134.0, 133.3, 132.5, 129.0, 128.8, 128.0, 127.6, 127.0, 126.2, 125.4, 124.2, 123.0, 122.2, 121.5, 120.0, 118.8, 117.6, 111.3, 108.5, 102.1. HRMS calcd for $C_{23}H_{16}BrN_5O$ 457.0538 found 457.0525. IR (KBr) $\nu_{max}$: 1693 $cm^{-1}$.

**Biological materials and methods**

***Reagents and antibodies***

SDF-1α and [$^{125}$I]-SDF-1α were obtained from Sichim and Perkin-Elmer, respectively. Antibodies used for immunoblotting were: total Akt, phosphoAkt$^{Ser437}$ and GAPDH (Santa Cruz Biotechnology), MAPK and phosphoMAPK$^{Thr202/Tyr204}$ (Cell Signaling Technology). Peroxidase-coupled secondary antibodies goat anti-mouse or anti-rabbit were obtained from Santa Cruz Biotechnology and the enhanced chemiluminescence system was from Amersham Pharmacia. Collagenase, 3-[4,5-Dimethylthiazol-2-yl]-2,5-diphenyltetrazolium bromide reagent/MTT and Coomassie Brilliant Blue were obtained from Sigma. TRIZOL reagent was from Invitrogen. RETROscript kit was purchased from Promega.

***Cell culture***

MCF-10A normal breast epithelial cells were grown in Dulbecco's modified Eagle's medium-F12 plus glutamax containing 5% Horse Serum, 1 mg/ml penicillin–streptomycin, 0.5 mg/ml hydrocortisone, and 10mg/ml insulin. Human estrogen receptor (ER)-negative MDA-MB-231 breast cancer cells were cultured in DMEM medium supplemented with 10% Fetal Bovine Serum, 0.1 nmol/L nonessential amino acid, 2 mmol/L L-glutamine, and 50 units/ml penicillin/streptomycin. Human ER-positive MCF-7 breast cancer cells were cultured in DMEM/F-12 medium supplemented with 5% Newborn Calf Serum, 0.1 nmol/L nonessential amino acid, 2 mmol/L L-glutamine, and 50 units/ml penicillin/streptomycin. Tamoxifen-resistant (TR) cells derived from MCF-7 cultured with 4-OH-tamoxifen over a period of 12 months and long-term estrogen-deprived cells (LTED) were derived from MCF-7 after six-month estrogen deprivation were obtained as previously described [28]. Subconfluent cell cultures, synchronized for 48 hours in medium without phenol red and serum, were used for all experiments.

***CAF isolation and conditioned medium systems***

Human cancer-associated fibroblasts (CAFs) were obtained from three specimen of human primary breast cancers as described [29]. Briefly, following digestion of small tumor pieces (collagenase 500 U/mL in Hank's balanced salt solution, at 37°C for 2 hours) and differential centrifugation (90 g for 2 minutes), the supernatant containing CAFs was centrifuged (500 g for 8 minutes), resuspended, and cultured in RPMI-1640 medium supplemented with 15% Fetal Bovine Serum, and antibiotics. CAFs between 4-10 passages

were used, tested by mycoplasma-presence, authenticated by morphology and FAP and α-SMA expression. For generation of conditioned media, CAFs were incubated with medium without phenol red and serum for 48-72 hours. Conditioned media were collected, centrifuged to remove cellular debris and utilized in respective experiments.

***RT-PCR assays***

Total cellular RNA was extracted using TRIZOL reagent as suggested by the manufacturer. The purity and integrity were checked spectroscopically and by gel electrophoresis before carrying out the analytical procedures. Two microgram of total RNA were reverse transcribed in a final volume of 20 µL using a RETROscript kit as suggested by the manufacturer. The cDNAs obtained were amplified by PCR using the following primers: 5'-TTACCCGCAAAAGACAAGT-3' (SDF1-α forward) and 5'-AGGCAATCACAAAACCCAGT-3' (SDF1-α reverse), 5'-AATCTTCCTGCCCACCATCT-3' (CXCR4 forward) and 5'-GACGCCAACATAGACCACCT-3' (CXCR4 reverse), 5'-CTCAACATCTCCCCCTTCTC-3' (36B4 forward) and 5'-CAAATCCCATATCCTCGTCC-3' (36B4 reverse). Negative controls containing water instead of first strand cDNA were utilized.

***Wound-healing assays***

For the measurement of cell migration during wound healing, confluent cell cultures were incubated in phenol-red and serum-free medium for 24 hours before the beginning of the experiment. Cell monolayers were then scraped, washed to remove debris and treated as indicated in the respective experiments. Wound closure was monitored over 24 hours. Cells were then fixed, stained with Comassie Brillant Blue and photographed after wounding under phase contrast microscopy at 10X magnification. Pictures represent one of three-independent experiments.

***Cell proliferation assays***

*MTT assays.* Cells (2 x $10^4$ cells/well) were plated in 24-well plates and treated as indicated for 3 days. The MTT assay was performed as the following: 100 µL MTT solution in PBS (2 mg/mL) was added into each

well and allowed to incubate at 37°C for 2 hours followed by media removal and solubilization in 500 µL dimethyl sulfoxide (DMSO). After shaking the plates for 15 minutes, the absorbance at 570 nm was measured in each well, including the blanks. Cell proliferation was expressed as fold change relative to vehicle-treated cells. A minimum of three experiments, containing eight different doses of FIL2 in triplicate, was combined for $IC_{50}$ calculations. The absorbance readings were used to determine the $IC_{50}$ using GraphPad Prism 4 (GraphPad Software). Briefly, values were log-transformed, normalized, and nonlinear regression analysis was used to generate a sigmoidal dose– response curve to calculate $IC_{50}$ values.

*Soft agar growth assays.* Cells ($10^4$/well) were plated in 0.35% agarose with 5% charcoal stripped-FBS in phenol red-free media (4 mL), with 0.7% agarose base in six-well plates. After two days, media containing vehicle or indicated treatments were added to the top layer, and replaced every 2 days. After 14 days, 300 µL of MTT reagent was added to each well and incubated at 37°C for 4 hours. Plates were then placed at 4°C overnight and colonies > 50µm diameter from triplicate assays were counted. The data are representative of three independent experiments, each performed in triplicates.

***Immunoblot analysis***

Total protein lysates were subjected to SDS–PAGE as described [30]. Briefly, cells were harvested in cold PBS and resuspended in lysis buffer containing HEPES (20 mmol/L, pH 8), EGTA (0.1 mmol/L), $MgCl_2$ (5 mmol/L), NaCl (0.5M), glycerol (20%), Triton (1%), and protease inhibitors (0.1 mmol/L sodium orthovanadate, 1% phenylmethylsulfonylfluoride, and 20 mg/mL aprotinin). Equal amounts of total protein lysates were resolved on a 11% SDS–polyacrylamide gel, transferred to a nitrocellulose membrane, and probed with appropriate antibodies as indicated in the respective experiments. Band intensities representing relevant proteins were measured by Scion Image laser densitometry scanning program (Scion Corporation) and standard deviations along with associated P values for the biological replicates were determined by using GraphPad-Prism4 software (GraphPad Inc., San Diego, CA). Immunoblots show one representative image of three separate experiments.

***[$^{125}$I]-SDF-1α competition binding assays***

MDA-MB-231 cells were harvested with versene reagent and washed twice in PBS. Ligand binding experiments were performed using 1 nM of [$^{125}$I]-SDF-1α (specific activity, 2.200 Ci/mmol) in a final volume of 100 µL binding buffer (50 mM HEPES, pH 7.4, 1 mM $CaCl_2$, 150 mM NaCl, 5 mM $MgCl_2$, 5% bovine serum albumin) containing 5 x $10^5$ cells/well in the presence of serially diluited concentrations of unlabeled SDF-1α or FIL2 compound. Nonspecific binding was determined by adding 150 nM of unlabeled SDF-1α. Samples were incubated for 60 minutes at 4°C. After incubation, cells were washed twice with 300 µL wash buffer (50 mM HEPES, pH 7.4, 1 mM $CaCl_2$, 500 mM NaCl, 5 mM $MgCl_2$). Bound ligands were determined by standard gamma counting techniques. At least three independent experiments were performed. The binding data were analyzed by nonlinear regression using the GraphPad PRISM program.

***Statistical analysis***

Data were analyzed for statistical significance using two-tailed student's Test, GraphPad-Prism4 software. Standard deviations (S.D.) were shown.

## RESULTS AND DISCUSSION

### Design and synthesis

The isothiourea ligand IT1t (**4**), [(E)-(6,6-dimethyl-5,6-dihydroimidazo[2,1-b]thiazol-3-yl)methyl N,N'-dicyclohexylcarbamimidothioate dihydrochloride], showing an $IC_{50}$ = 48 nM in CXCR4 radioligand binding assay, was fruitfully used during the mapping of the active binding site of the protein, as already mentioned [20].

The rationale behind the design of the hereby-reported inhibitors was guided by two considerations: *in silico* analysis of the interactions between IT1t and CXCR4 in the crystal complex and the synthetic feasibility of the newly designed compounds using established procedures. In particular, we were interested in a chemical scaffold we could easily prepare using our recently reported method [27]. All the compounds designed using these criteria were docked and their binding mode analyzed to verify how well the new structures would mimic the IT1t binding mode (**Figure 3**). The first designed modification for the backbone of the new compounds was the replacement of the dihydroimidazo[2,1-*b*]thiazole system of IT1t with a flatter *N*-

substituted indole that could still result in favorable interactions with Trp94. The 6,6-dimethyl motif is replaced by a bromine atom directed towards the Tyr116 and filling the small hydrophobic cavity present in that position. The benzo group linked at position 1 of indole could at the same time establish additional hydrophobic interactions with Val112 and support the polar carbohydrazide moiety. This latter group is also establishing a hydrogen bond with Asp97, a residue that is involved in a strong interaction with the carbamimidic group of IT1t. The final modification was the removal of bulky cyclohexyl substituents of IT1t with the concomitant introduction of a cyclic system linked to the N'-atom of the benzohydrazide moiety. Among the attempted aryl substituents, the pyrazine gave best results probably due to the possibility to interact further with Arg183 (**Figure 3B**).

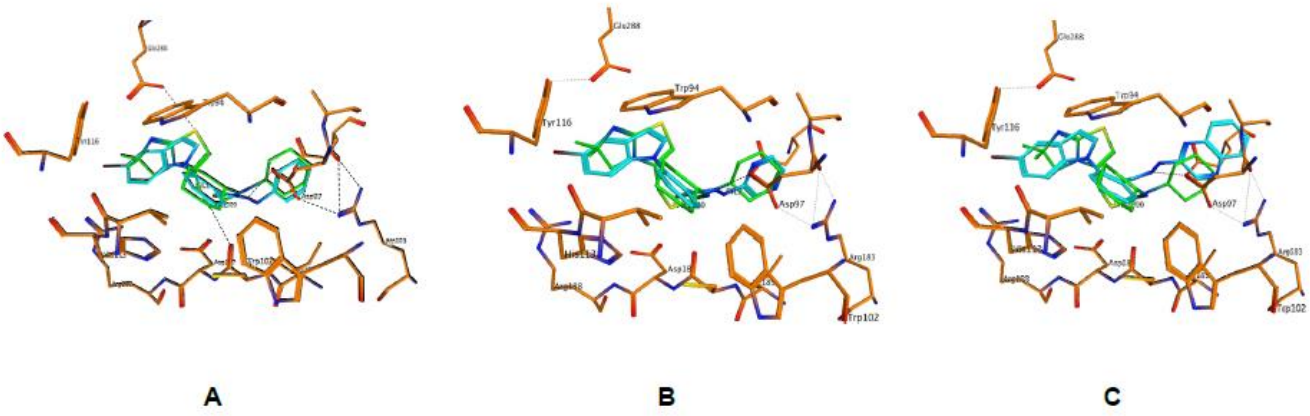


**Figure 3. Docking simulation.** Putative binding mode of **(A)** FIL1, **(B)** FIL2 and **(C)** FIL3 (represented in cyan) in the CXCR4 binding pocket. Co-crystallized ligand (IT1t) is represented in green.

The three studied compounds (FIL 1-3) were obtained in moderate yields starting from a common intermediate, the 2-(5-bromo-1*H*-indol-1-yl)benzoic acid **1,** whose preparation was recently described [27]. The acid **1** was coupled with a proper hydrazine derivative by action of 1,1'-carbonyldiimidazole (CDI) in DMF to give compounds FIL1, FIL2 and FIL3 in 22, 50 and 37% yield, respectively (**Figure 4**).

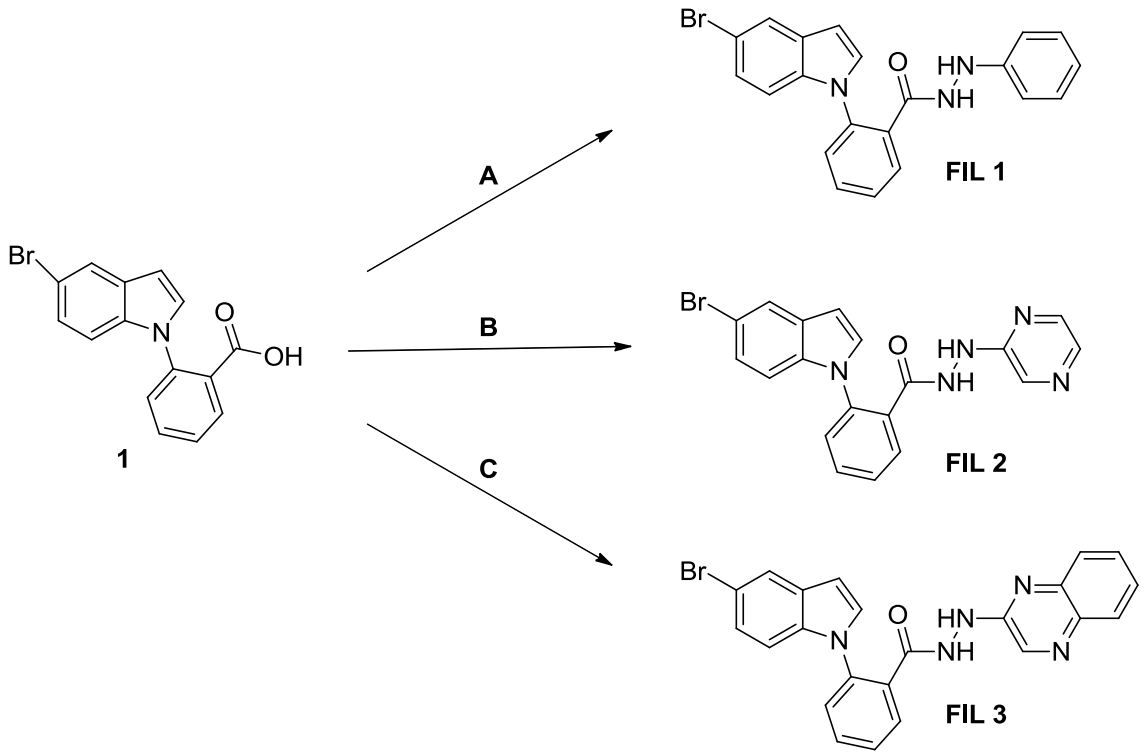


**Figure 4. Synthesis of FIL 1-3**. Reagents and Conditions: (**A**) CDI, DMF, phenylhydrazine, 60°C (22%); (**B**) CDI, DMF, 2-hydrazinylpyrazine, 60°C (50%); (**C)** CDI, DMF, 2-hydrazinylquinoxaline, 60°C (37%).

**FIL2 compound blocks SDF-1α-dependent cell motility, proliferation and downstream signalling activation in MDA-MB-231 breast cancer cells**

It has been reported that the chemokine SDF-1α and its cognate receptor CXCR4 are expressed in breast carcinoma tissues and in breast cancer cell lines, and that cell clones isolated from metastatic sites (e.g., bone or lungs) exhibit higher levels of CXCR4 than the parental cells [31-33]. Prior to evaluating the biological activity of the CXCR4 antagonists, we analyzed SDF-1α and CXCR4 expression in estrogen receptor (ER)-negative MDA-MB-231 breast cancer cells, which are well characterized in terms of their metastatic potential and properties. RT-PCR analysis revealed SDF-1α and CXCR4 expression in MDA-MB-231 breast cancer cells (**Figure 5A**). Given the crucial role of SDF-1α/CXCR4 signaling axis in modulating cancer cell migration [34], we first explored the ability of the CXCR4 antagonists that we synthesized to inhibit cell motility in wound-healing assays. MDA-MB-231 breast cancer cells were treated with three different CXCR4 antagonists (FIL1, FIL2, FIL3) at increasing concentrations (0.01, 0.1, 1, 10μM) for 24 hours. **Figure 5B** showed that FIL1 and FIL3 did non affect cell motility at all the doses tested, while FIL2 was

able to inhibit migration at concentrations as low as 10nM. Therefore, in agreement with the docking simulation, the *in vitro* evaluations of the CXCR4 inhibitory efficacy on cell motility also resulted in the selection of the antagonist FIL2 for the subsequent studies. Next, we assessed the effects of increasing concentrations of FIL2 compound on breast cancer cell proliferation (**Figure 5C**). We observed that FIL2 treatment for 72 hours significantly reduced cell viability in MDA-MB-231 cells at all the doses tested, with IC50 values of 49.4 µM (95% Confidence Intervals, 30.1-81.2 µM). The activity of FIL2 compound was also evaluated using soft agar anchorage-independent growth. Consistently with MTT assays, FIL2 treatment decreased colony formation in MDA-MB-231 cells (**Figure 5D**). In contrast, FIL2 did not elicit any significant growth inhibitory effects on MCF-10A non-tumorigenic breast epithelial cells (**Figure 5E**). Taken together, these results showed that the compound FIL2 inhibits cell growth and migratory potential of highly invasive MDA-MB-231 breast cancer cells, interfering with the autocrine effects of SDF-1α /CXCR4 system in these cells.

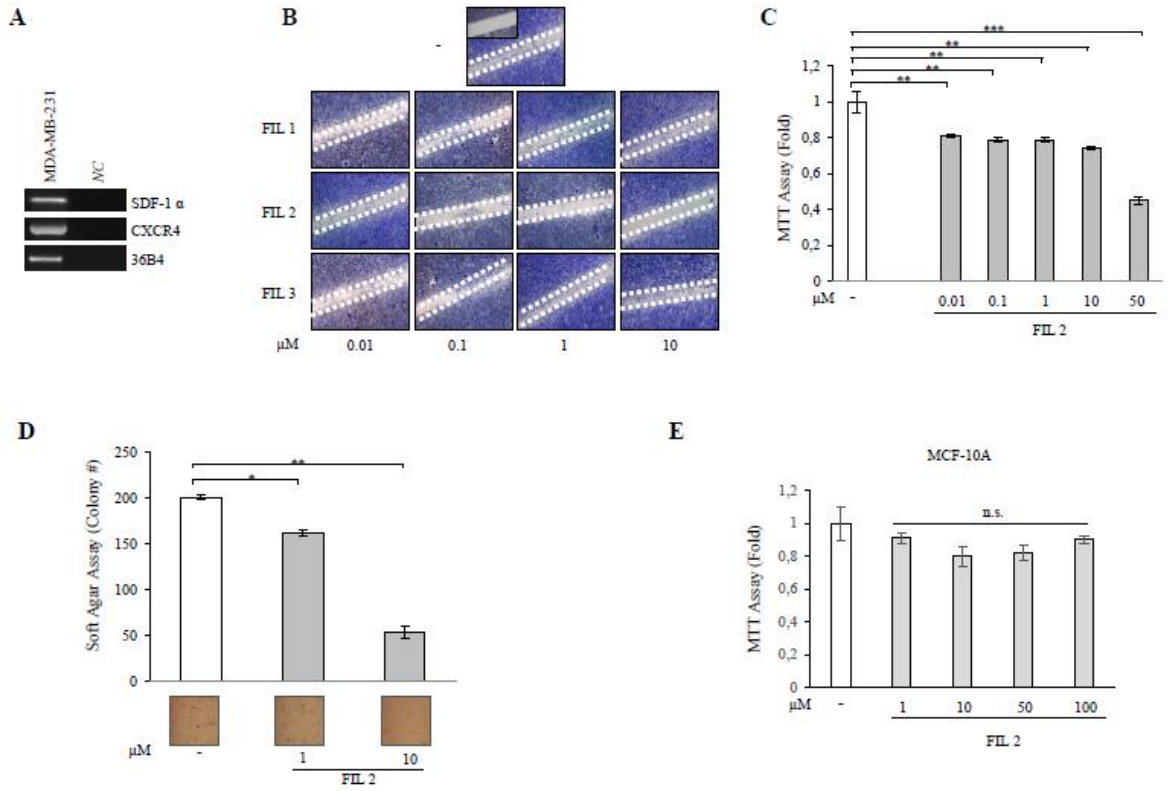


**Figure 5. FIL2 compound inhibits motility and growth of MDA-MB-231 breast cancer cells**. **(A)** RT-PCR for SDF-1α, CXCR4 and 36B4 (internal standard). *NC*, negative-control. **(B)** Wound-healing assay in cells treated with vehicle (-) or increasing concentrations of FIL1, FIL2 and FIL3 compounds (0.01, 0.1, 1, 10µM). *Small squares*, time 0. **(C)** MTT growth assay in cells treated with vehicle (-) or FIL2 compound (0.01, 0.1, 1, 10, 50 µM). **(D)** Soft agar

anchorage-independent growth assay in cells treated with vehicle (-) or FIL2 compound (1, 10µM). *Bottom panel*, a typical well for each condition is shown. **(E)** MTT growth assay in MCF-10A normal epithelial breast cells treated with vehicle (-) or FIL2 compound (1, 10, 50, 100 µM). n.s.= non significant. **P*<0.05, ***P*<0.005, ****P*<0.0005.

In order to verify that the CXCR4 antagonist FIL2 binds to the CXCR4 receptor, we established a whole cell-based [$^{125}$I]-SDF-1α ligand competition binding assay. A typical result is shown in **Figure 6**. In a homologous competition binding assay, we found that MDA-MB-231 cells bind SDF-1α in a dose dependent-manner with $IC_{50}$ value of 26.1 ± 8 nmol/L (**Figure 6A**). The [$^{125}$I]-SDF-1α binding was replaced by cold SDF-1α, confirming the specificity of SDF-1 binding. FIL2 was able to inhibit [$^{125}$I]-SDF-1α ligand binding to MDA-MB-231 cells in a heterologous competition binding assay with $IC_{50}$ value of 10.9 ± 4.2 nmol/L (**Figure 6B**). The binding curve was fitted to an one site binding model. These results indicate that FIL2 exhibits an increased affinity for the receptor compared to endogenous SDF-1α ligand and may act as a highly selective CXCR4 receptor antagonist.

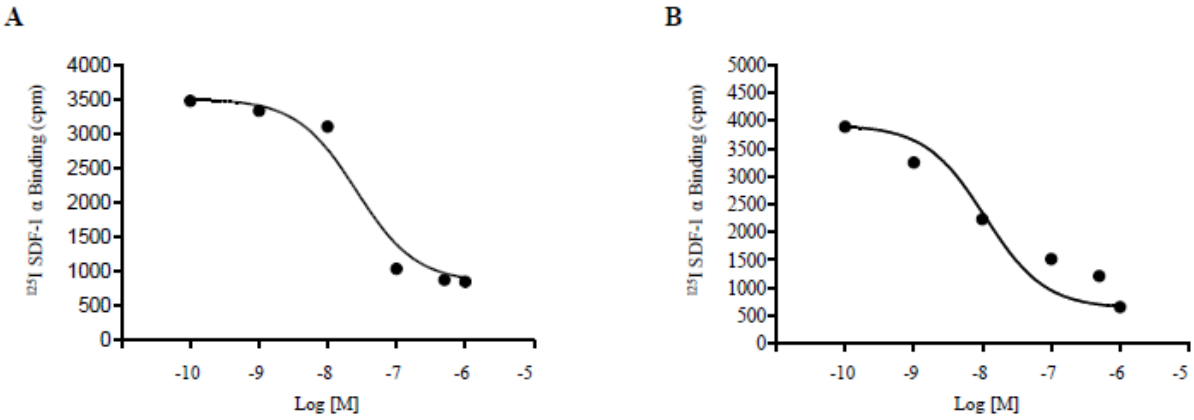


**Figure 6. [$^{125}$I]-SDF-1α ligand binding by MDA-MB-231 cells.** [$^{125}$I]-SDF-1 competition binding assay was performed as described in Materials and Methods section. [$^{125}$I]-SDF-1α bound to MDA-MB-231 cells was competed with either unlabelled SDF-1α **(A)** or FIL2 compound **(B)**. The specificity of [$^{125}$I]-SDF-1α binding was confirmed by a replacement experiment with cold SDF-1α (150-fold excess).

We, then, aimed to assess the ability of FIL2 compound to counteract SDF-1α-induced cell motility and growth. As expected, MDA-MB-231 breast cancer cells moved the farthest in either direction to close the 'gap' in the cell bed after treatment with SDF-1α (200 ng/mL) compared to basal vehicle-treated conditions. Pretreatment with FIL2 at 0.01-1μM concentrations strongly reduced SDF-1α-mediated effects on cell motility (**Figure 7A**). Moreover, FIL2 exposure significantly reduced the increase in the colony numbers observed after SDF-1α treatment (**Figure 7B**).

Stimulation of CXCR4 by SDF-1 induces phosphorylation of Akt and p42/44 MAPK, promoting proliferation and migration of different types of cells [35]. Thus, we conducted time-course studies to analyze whether FIL2 compound was able to antagonize the effects of SDF-1α on activation of the above mentioned downstream signaling molecules (**Figure 7C&7D**). As expected, treatment with SDF-1α resulted in an increased phosphorylation of Akt and MAPK in MDA-MB-231 breast cancer cells. Interestingly, pretreatment with FIL2 abrogated the SDF-1α activation of these signaling pathways.

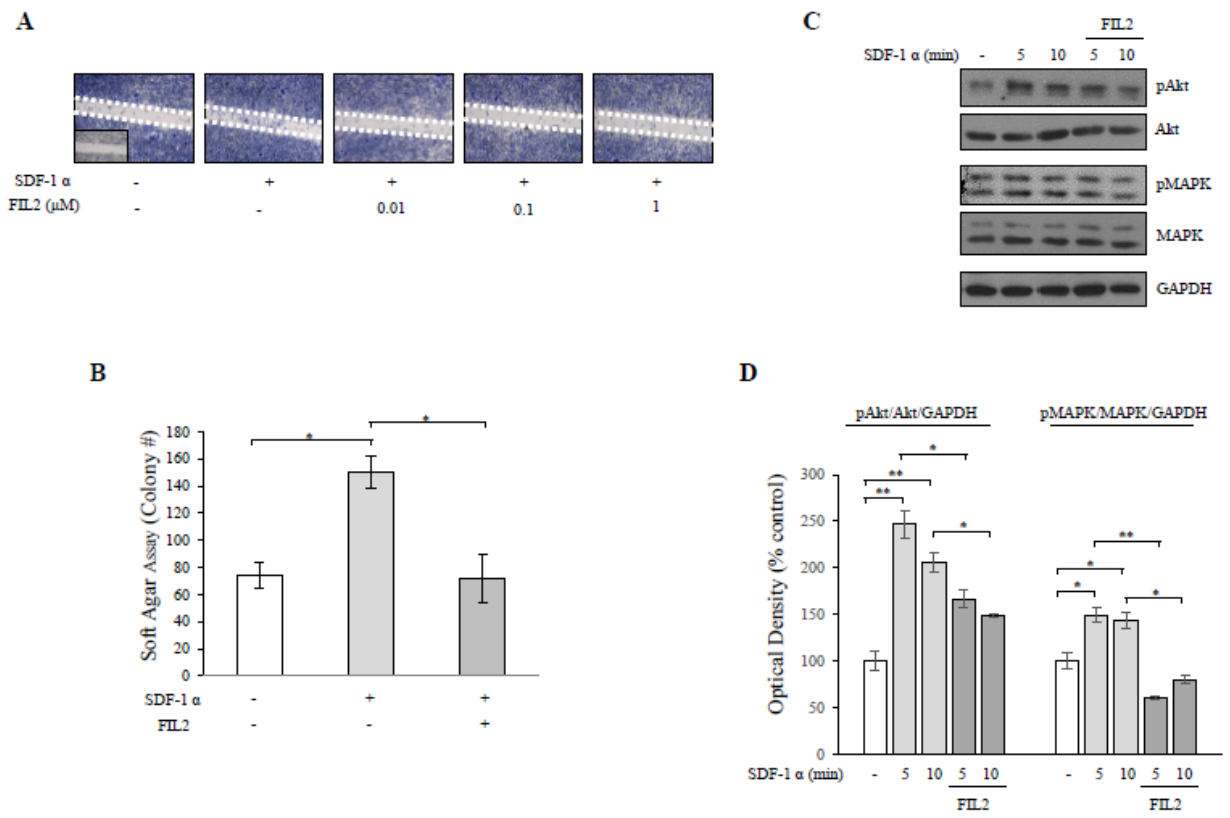


**Figure 7. FIL2 compound antagonizes SDF-1α–mediated motility, growth and signalling activation in MDA-MB-231 breast cancer cells**. **(A)** Wound-healing assay in cells treated with vehicle (-), SDF-1α (200 ng/mL) with or without FIL2 compound (0.01, 0.1, 1μM). *Small squares*, time 0. **(B)** Soft agar anchorage-independent growth assay in cells treated with vehicle (-), SDF-1α (200 ng/ml) in the presence or not of FIL2 compound (1μM). **(C)** Immunoblotting

of phosphorylated (p) Akt and MAPK and total proteins from cells treated with SDF-1 (200 ng/mL for 5 and 10 minutes) with or without FIL2 compound (1μM). **(D)** Histograms represent the mean ± SD of three separate experiments in which band intensities were evaluated in terms of optical density arbitrary units and expressed as percentage of control which was assumed to be 100%. **P*<0.05, ***P*<0.005.

**Efficacy of FIL2 compound in antagonizing CXCR4 signaling in different breast cancer cell models and co-culture systems**

To extend our results, as additional model system for breast cancer we investigated the effects of FIL2 molecule in affecting growth, and motility of ER-positive MCF-7 breast cancer cells. First, we demonstrated SDF-1α and CXCR4 expression in these cells (**Figure 8A**). As previously shown for MDA-MB-231 cells, we found a significant decrease in both anchorage-independent proliferation and migration of MCF-7 breast cancer cells after FIL2 exposure (**Figure 8B**). Again, treatment with SDF-1 at 200 ng/mL concentration increased colony numbers and motility of cells, and pretreatment with FIL2 compound reduced SDF-1α-mediated activities (**Figure 8C**). Finally, we demonstrated that FIL2 was able to reverse the stimulatory effects induced by SDF-1α on the phosphorylation levels of Akt and MAPK (**Figure 8D&8E**), confirming that the FIL2 compound may act as a CXCR4 antagonist in different breast cancer cellular backgrounds.

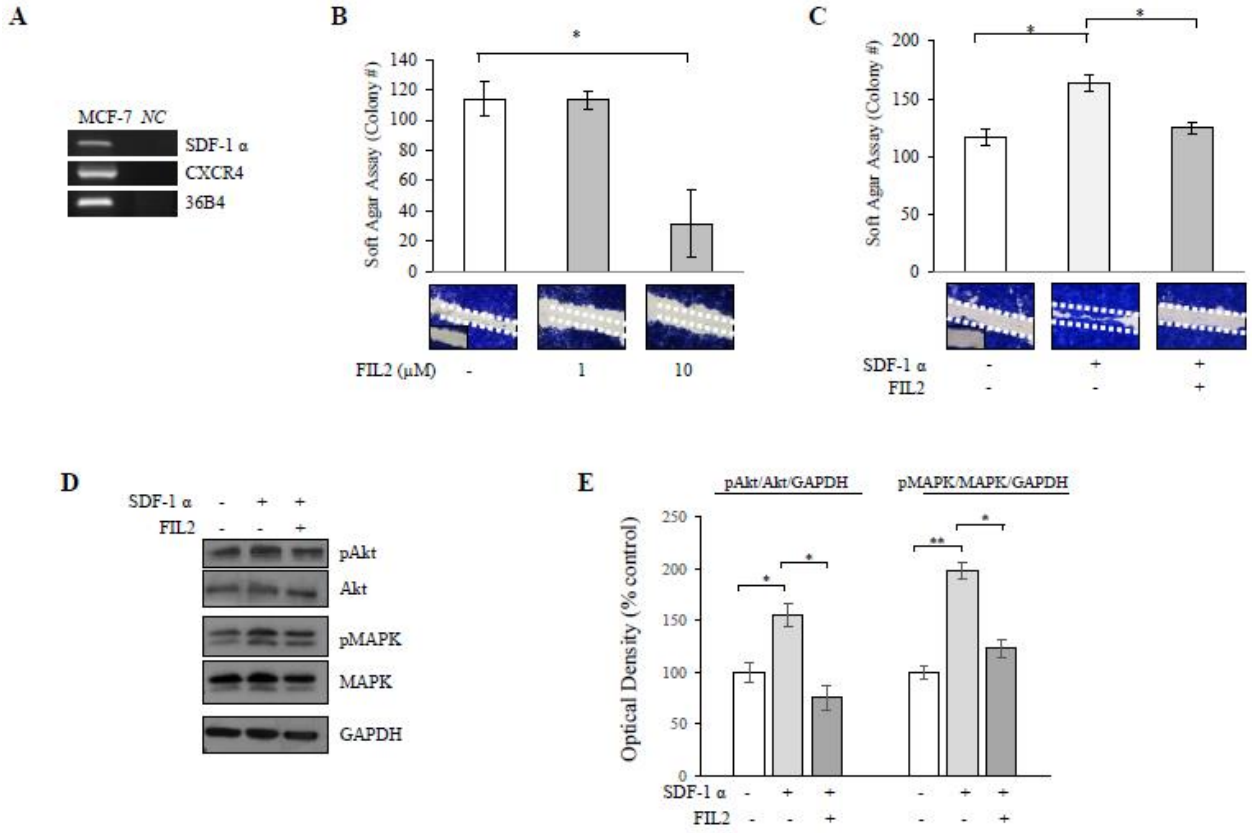


**Figure 8. FIL2 effects in MCF-7 breast cancer cells**. **(A)** RT-PCR for SDF-1α, CXCR4 and 36B4 (internal standard). *NC*, negative-control. **(B)** Soft agar anchorage-independent growth (*upper panel*) and wound-healing (*lower panel*) assays in cells treated with vehicle (-) or FIL2 compound (1, 10μM). *Small squares*, time 0. **(C)** Soft agar anchorage-independent growth (*upper panel*) and wound-healing (*lower panel*) assays in cells treated with vehicle (-), SDF-1α (200 ng/mL) with or without FIL2 compound (1μM). *Small squares*, time 0. **(D)** Immunoblotting of phosphorylated (p) Akt and MAPK and total proteins from cells treated with SDF-1α (200 ng/mL for 5 minutes) with or without FIL2 compound (1μM). Numbers below the blots represent the average fold change in phospho-proteins/total proteins/GAPDH ratio relative to vehicle (-)-treated cells. **(E)** Histograms represent the mean ± SD of three separate experiments in which band intensities were evaluated in terms of optical density arbitrary units and expressed as percentage of control which was assumed to be 100%. **P*<0.05, ***P*<0.005.

The behavior of tumor cells seems to be regulated not only by cell autonomous signals, but it also relies on heterotypic signals coming from surrounding myofibroblast stromal cells, able to create a specific and local microenvironment to tightly control breast cancer proliferation and differentiation. Indeed, fibroblasts adjacent to primary breast tumors have higher expression of SDF-1α than those of normal breast tissue and through this paracrine signaling, CXCR4 may promote local tumor cell proliferation, motility, and invasion [36,37]. Therefore, we examined the ability of FIL2 compound to inhibit breast cancer cell proliferation and motility promoted by cancer-associated fibroblasts (CAFs). To this aim, CAFs were isolated from biopsies of primary breast tumors and coculture experiments were performed to create 'in vitro' conditions that can

mimic the complex 'in vivo' microenvironment [29,38]. Both MDA-MB-231 and MCF-7 breast cancer cells were incubated with phenol-red and serum-free medium (-), or CAF-derived conditioned media (C.M.) in the presence or not of FIL2 compound and growth and motility were evaluated (**Figure 9**). As previously demonstrated [29], CAF C.M. significantly increased colony numbers and motility of breast cancer cells. Interestingly, treatment with FIL2 compound attenuated growth and migration-promoting activities of CAF C.M.

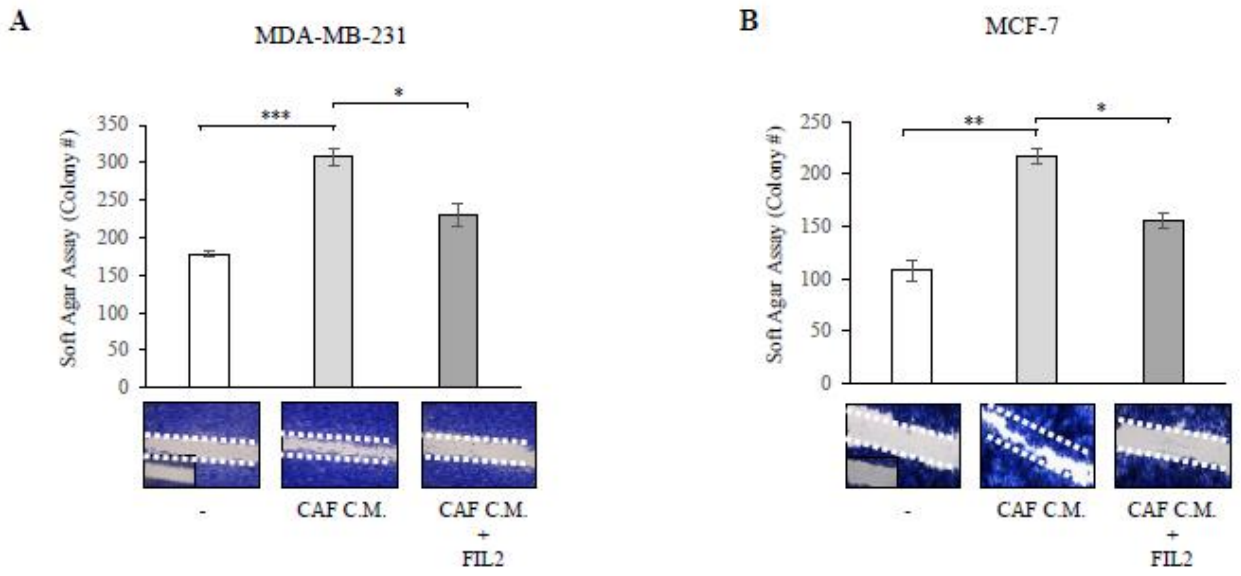


**Figure 9. FIL2 reduces growth and migration induced by CAF-derived conditioned media in breast cancer cells**. Soft agar anchorage-independent growth (*upper panel*) and wound-healing (*lower panel*) assays in MDA-MB-231 **(A)** and MCF-7 **(B)** cells treated with phenol-red and serum-free medium (-), conditioned media derived from CAFs (CAF C.M.) with/without FIL2 compound (1μM). *P<0.05, **P<0.01, ***P<0.0005. Small squares, time 0.

It has been recently reported that enhanced CXCR4 signaling is sufficient to drive ER-positive breast cancers to an endocrine therapy-resistant phenotype, highlighting CXCR4 signaling as a rational therapeutic target also for the treatment of ER-positive, estrogen-independent breast carcinoma [39,40]. Therefore, as a final step of this study, we evaluated whether FIL2 compound was able to affect the progression of hormone-independent and therapeutic-resistant breast cancer cell lines, using other two additional breast cancer cellular models. In particular, as experimental cell models for acquired resistance, we used: 1) tamoxifen-resistant (TR) cells obtained from MCF7 cells cultured with 4-OH tamoxifen over a period of 12 months; 2) MCF7 LTED cells, which gradually acquired aromatase inhibitor resistance upon culture in estrogen/steroid-

free conditions [28]. As shown in **Figure 10A&10B**, we found increased SDF-1α and CXCR4 expression in TR cells and LTED cells compared to parental MCF-7 breast cancer cells. In agreement with a previous study [30], resistant cells exhibited a higher basal non-stimulated growth and motility (**Figure 10C&10D**). Treatment with SDF-1α or CAF-derived conditioned medium resulted in an enhancement of growth and motility of TR and LTED cells and, again, FIL2 compound had a significant inhibitory effect in basal as well as SDF-1α and C.M.-stimulated conditions.

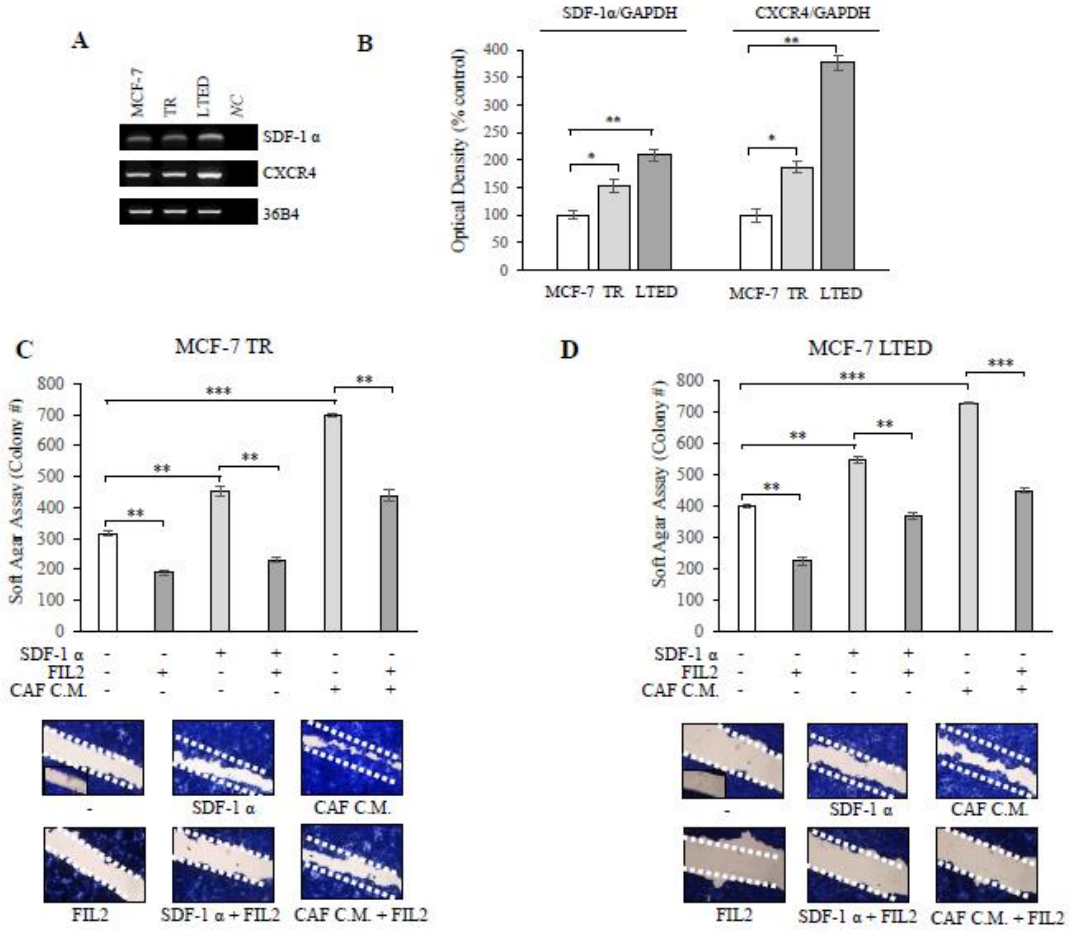


**Figure 10. FIL2 compound reduces growth and migration in hormone-resistant breast cancer cells**. **(A)** RT-PCR for SDF-1α, CXCR4 and 36B4 (internal standard). *NC*, negative-control. **(B)** Histograms represent the mean ± SD of three separate experiments in which band intensities were evaluated in terms of optical density arbitrary units and expressed as percentage of control, which was assumed to be 100%. Soft agar anchorage-independent growth (*upper panel*) and wound-healing (*lower panel*) assays in tamoxifen-resistant MCF-7 TR **(C)** and long term-estrogen deprived MCF-7 LTED **(D)** breast cancer cells treated with vehicle (-), SDF-1α (200 ng/mL), conditioned media derived from CAFs (CAF C.M.) with or without FIL2 compound (1μM). *P<0.05, **P<0.005, ***P<0.0005. *Small squares*, time 0.

## CONCLUSION

CXCR4 plays a role in several pathophysiological conditions such as cancer, altered immune conditions and HIV infection, hence chemical agents able to prevent the interaction between this receptor and its endogenous ligand SDF-1 might result useful in the management of a number of pathologies [5-9]. Despite the huge number of identified CXCR4 antagonists, most of them show inadequate bioavailability, that represents the bigger limit to a clinical application. Thus, only a few compounds have so far entered clinical trials [11-15]. Among the small-molecule antagonists, indole based compounds, suitably modified, seem to meet pharmacokinetic requirements and optimal features to interact with the target.

In the present study, we describe the design and the synthesis of three novel molecules namely FIL1-3 investigated for their capability to interact with CXCR4. In particular, one of the derivatives shows the ability to bind to CXCR4 as revealed by molecular docking and whole cell-based [$^{125}$I]-SDF-1α ligand competition binding assays. This compound is able to inhibit SDF-1α-mediated cell motility, proliferation and downstream signaling activation in different breast cancer cell lines as well as to prevent tumor microenvironment stimulatory effects in co-culture studies. This activity assumes a great importance in hormone-resistant breast cancer cell lines, as resistance to endocrine therapy still remains a major clinical concern.

Since breast cancer progression has been correlated to the SDF-1α-CXCR4 signaling axis, specific agents able to prevent this interaction, could result of great interest for the management of such a type of cancer.

Based on these findings, we may consider FIL-2 as a lead for the development of a new class of selective antagonist ligands of CXCR4 that may be useful in order to better assess the biological function of this receptor. In addition, the CXCR4 antagonism may represent a starting point for the development of novel therapeutics for the treatment of breast cancer and other diseases in which the receptor is involved.

## FUTURE PERSPECTIVE

The role played by the interaction of CXCR4 and its natural ligand SDF-1α in several types of tumors, including breast cancer, as well as in other diseases is clearly recognized. This suggests that CXCR4 represents a promising target for the development of innovative therapeutics and the identification of FIL2,

as a selective targeting CXCR4 lead compound, may help the discovery of effective CXCR4 antagonists to be proposed to clinical practice. Moreover, the possibility to prepare a FIL2 $^{79}$Br- or $^{81}$Br-radiolabeled derivative to be used as functional biomarkers in early diagnosis, disease prevention, and drug response may represent a further applicative development for the class of compounds herein described.

## EXECUTIVE SUMMARY

CXCR4 Inhibition

Inhibition of CXCR4 represents a promising therapeutic approach in the treatment of breast cancer and other diseases involving this receptor.

Lead identification and synthesis

A new selective CXCR4 antagonist has been identified and could be useful for a rational design of broad-spectrum therapeutics.

Binding assay

A whole cell-based [$^{125}$I]-SDF-1α ligand competition binding assay was accomplished in order to verify that FIL2 binds to the CXCR4 receptor as hypothesized by molecular docking prevision.

## DEFINED KEY TERMS

Docking simulation:

Computational simulation technique used to predict the binding orientation of a candidate ligand into the active site of the target protein.

Mapping of the active binding site:

The assignment of chemical features for the definition of topology in the interaction site of a receptor.

Poly-substituted indoles:

Molecules based on an indole scaffold bearing substituents capable to bind specific groups of the active site of a target molecule.

Acquired endocrine resistance:

Despite the significant advances in the treatment of breast cancer following the introduction of endocrine therapy (tamoxifen and aromatase inhibitors), in many estrogen receptor-positive breast tumors drug resistance develops during treatment leading to disease progression (acquired resistance).

Tumor microenvironment:

The behavior of malignant cells seems to be dependent not only on cell autonomous signals, but it also relies on heterotypic signalings deriving from surrounding stromal cells, able to generate a microenvironment to tightly control breast tumor progression. Among the stromal cells, cancer-associated fibroblasts (CAFs) play a crucial role in determining cancer proliferation and differentiation.

Soft agar growth assay:

The soft agar colony formation assay is a technique used to evaluate cellular anchorage-independent proliferation *in vitro*. This assay is considered to better reflect *in vivo* three-dimensional tumor growth.

Ligand binding assay:

Detection method used to evaluate the interactions that occur between two molecules, such as a receptor and its ligands.

Coculture experiments:

Coculture experiments were performed by incubation of breast cancer cells with CAF-derived conditioned media. This allows to create *in vitro* conditions that can mimic the complex *in vivo* microenvironment.

**ACKNOWLEDGEMENTS**

This work was supported by AIRC Grant (IG11595) to SA. European Commission/FSE/Regione Calabria to FC.

REFERENCES

1 Lefrancois M, Lefebvre MR, Saint-Onge G *et al*. Agonists for the chemokine receptor CXCR4. *ACS Med. Chem. Lett.* 2, 597-602 (2011).

2 Allen SJ, Crown SE, Handel TM. Chemokine: receptor structure, interactions, and antagonism. *Annu. Rev. Immunol.* 25, 787-820 (2007).

3 Bleul CC, Wu L, Hoxie JA, Springer TA, Mackay CR. The HIV coreceptors CXCR4 and CCR5 are differentially expressed and regulated on human T lymphocytes. *P. Natl. Acad. Sci. USA* 94, 1925-1930 (1997).

4 Bleul CC, Farzan M, Choe H *et al*. The lymphocyte chemoattractant SDF-1 is a ligand for LESTR/fusin and blocks HIV-1 entry. *Nature* 382, 829-833 (1996).

5 Raman D, Sobolik-Delmaire T, Richmond A. Chemokines in health and disease. *Exp. Cell. Res.* 317, 575-589 (2011).

6 Balkwill FR. The chemokine system and cancer. *J. Pathol.* 226, 148-157 (2012).

7 Didigu CA, Doms RW. Novel Approaches to Inhibit HIV Entry. *Viruses* 4, 309-324 (2012).

8 Grande F, Garofalo A, Neamati N. Small molecules anti-HIV therapeutics targeting CXCR4. *Curr. Pharm. Des.* 14, 385-404 (2008).

**°Summarizes chemical classes of compounds able to prevent CXCR4-mediated HIV entry.**

9 Debnath B, Xu S, Grande F, Garofalo A, Neamati N. Small molecule inhibitors of CXCR4. *Theranostics* 3, 47-75 (2013).

**°°Summarizes all classes of compounds targeting CXCR4.**

10 Burger JA, Stewart DJ. CXCR4 chemokine receptor antagonists: perspectives in SCLC. *Expert Opin. Investig. Drug.* 18, 481-490 (2009).

11 [Internet] NCT01339039. Plerixafor (AMD3100) and Bevacizumab for recurrent high-grade glioma. http://clinicaltrialsgov.

12 [Internet] NCT01141543. Feasibility and efficiency study of leukemic cell mobilization with Plerixafor injection. http://clinicaltrialsgov.

13 [Internet] NCT01373229. Lenalidomide + Plerixafor in previously treated chronic lymphocytic leukemia (CLL). http://clinicaltrialsgov.

14 [Internet] NCT01058993. AMD 3100 for treatment of myelokathexis. http://clinicaltrialsgov.

15 [Internet] NCT01018979. Safety, pharmacokinetics and stem cell mobilization of TG-0054 in multiple myeloma, non-Hodgkin lymphoma and Hodgkin disease patients. http://clinicaltrialsgov.

16 Harvey JR, Mellor P, Eldaly H, Lennard TW, Kirby JA, Ali S. Inhibition of CXCR4-mediated breast cancer metastasis: a potential role for heparinoids? *Clin. Cancer Res*. 13, 1562-1570 (2007).

17 Wilson LJ, Liotta DC. Emergence of small-molecule CXCR4 antagonists as novel immune and hematopoietic system regulatory agents. *Drug Develop. Res.* 72, 598-602 (2011).

18 [Internet] NCT00089466. Safety and activity of the oral HIV entry inhibitor AMD11070 in HIV infected patients. http://clinicaltrialsgov.

19 Ueda S, Kato M, Inuki S *et al*. Identification of novel non-peptide CXCR4 antagonists by ligand-based design approach. *Bioorg. Med. Chem. Lett.* 18, 4124-4129 (2008).

20 Wu B, Chien EY, Mol CD *et al*. Structures of the CXCR4 chemokine GPCR with small-molecule and cyclic peptide antagonists. *Science* 330, 1066-1071 (2010).

21 Thoma G, Streiff MB, Kovarik J *et al*. Orally bioavailable isothioureas block function of the chemokine receptor CXCR4 in vitro and in vivo. *J. Med. Chem*. 24, 7915-7920 (2008).

22 Hung TC, Lee WY, Chen KB, Chen CYC. Lead Screening for CXCR4 of the Human HIV Infection Receptor Inhibited by Traditional Chinese Medicine. *BioMed Research International* ID 809816 (2014).

23 Sobolik T, Su YJ, Wells S, *et al*. CXCR4 drives the metastatic phenotype in breast cancer through induction of CXCR2 and activation of MEK and PI3K pathways. *Mol. Biol. Cell* 25, 566-582 (2014).

24 Zhang Z, Ni C, Chen W *et al*. Expression of CXCR4 and breast cancer prognosis: a systematic review and meta-analysis. *BMC Cancer*, 14:49 (2014).

25 Maestro 9.3, Schrödinger, LLC, New York, NY, 2012. http://www.schrodinger.com.

26 Molecular Operating Environment (MOE 2012.10). Chemical Computing Group, Inc. Montreal, Quebec, Canada. www.chemcomp.com.

27 Grande F, Brizzi A, Garofalo A, Aiello F. Active manganese dioxide promoted cyclization of *ortho*-(1*H*-pyrrol-1-yl)aryl and heteroaryl carboxylic acids to 5*H*-pyrrolo[1,2-*a*][3,1]benzoxazin-5-one derivatives. *Tetrahedron* 69, 9951-9956 (2013).

28 Lombardo Y, Faronato M, Filipovic A, Vircillo V, Magnani L, Coombes RC. Nicastrin and Notch4 drive endocrine therapy resistance and epithelial to mesenchymal transition in MCF7 breast cancer cells. *Breast Cancer Res.* 16, R62 (2014).

29 Barone I, Catalano S, Gelsomino L *et al*. Leptin mediates tumor-stromal interactions that promote the invasive growth of breast cancer cells. *Cancer Res*. 72(6), 1416-1427 (2012).

°°**Reinforces the concept that blocking cancer–stromal cell communication may represent an effective strategy for targeted therapy of breast cancer.**

30 Gu G, Barone I, Gelsomino L *et al*. Oldenlandia diffusa extracts exert antiproliferative and apoptotic effects on human breast cancer cells through ERα/Sp1-mediated p53 activation. *J. Cell. Physiol.* 227(10), 3363-72 (2012).

31 Müller A, Homey B, Soto H *et al*. Involvement of chemokine receptors in breast cancer metastasis. *Nature* 410(6824), 50-56 (2001).

°**Highlights the involvement of CXCR4 in breast cancer spread and progression.**

32 Kang Y, Siegel PM, Shu W *et al*. A multigenic program mediating breast cancer metastasis to bone. *Cancer Cell* 3(6), 537-549 (2003).

33 Schmid BC, Rudas M, Resniczek GA, Leodolter S, Zeillinger R. CXCR4 is expressed in ductal carcinoma in situ of the breast and in atypical ductal hyperplasia. *Breast Cancer Res. Treat.* 84(3), 247-250 (2004).

34 Fernandis AZ, Prasad A, Band H, Klosel R, Ganju RK. Regulation of CXCR4-mediated chemotaxis and chemoinvasion of breast cancer cells. *Oncogene* 23, 157-167 (2004).

35 Kijowski J, Baj-Krzyworzeka M, Majka M *et al*. The SDF-1-CXCR4 axis stimulates VEGF secretion and activates integrins but does not affect proliferation and survival in lymphohematopoietic cells. *Stem Cells* 19, 453-466 (2001).

36 Allinen M, Beroukhim R, Cai L *et al*. Molecular characterization of the tumor microenvironment in breast cancer. *Cancer Cell*, 6, 17-32 (2004).

**°Outlines SDF-1 overexpression in tumor myoepithelial cells and myofibroblasts and its ability to bind to receptors on epithelial cells and enhance their proliferation, migration, and invasion.**

37 Orimo A, Gupta PB, Sgroi DC *et al*. Stromal fibroblasts present in invasive human breast carcinomas promote tumor growth and angiogenesis through elevated SDF-1/CXCL12 secretion. *Cell*, 121, 335-348 (2005).

**°Adds more insights in the role of SDF-1 as an important paracrine molecule in breast cancer microenvironment.**

38 Catalano S, Giordano C, Panza S *et al*. Tamoxifen through GPER upregulates aromatase expression: a novel mechanism sustaining tamoxifen-resistant breast cancer cell growth. *Breast Cancer Res. Treat.* 146(2), 273-285 (2014).

39 Rhodes LV, Short SP, Neel NF *et al*. Cytokine receptor CXCR4 mediates estrogen-independent tumorigenesis, metastasis, and resistance to endocrine therapy in human breast cancer. *Cancer Res.* 71, 603-613 (2011).

**°Underlines CXCR4 signaling as a rational therapeutic target for the treatment of estrogen-independent breast carcinomas**

40 Dubrovska A, Hartung A, Bouchez LC *et al*. CXCR4 activation maintains a stem cell population in tamoxifen-resistant breast cancer cells through AhR signalling. *Br. J. Cancer* 107(1), 43-52 (2012).